







Cite this: *Biomater. Sci.*, 2023, **11**, 2330

Received 10th September 2022,
Accepted 2nd March 2023

DOI: 10.1039/d2bm01471h

rsc.li/biomaterials-science

Laser-responsive sequential delivery of multiple antimicrobials using nanocomposite hydrogels†

Meera Patel, ‡^{a,b} Alexander L. Corbett,  §^{a,b} Aarushi Vardhan,^a Keuna Jeon, ^{a,b} Nesha May O. Andoy ^a and Ruby May A. Sullan ^{*a,b}

Precise control of antimicrobial delivery can prevent the adverse effects of antibiotics. By exploiting the photothermal activity of polydopamine nanoparticles along with the distinct transition temperatures of liposomes, a near-infrared (NIR) laser can be used to control the sequential delivery of an antibiotic and its adjuvant from a nanocomposite hydrogel—preventing bacterial growth.

Systemic antibiotic therapy, though highly beneficial in controlling bacterial infections, comes with adverse effects. The indiscriminate use of antibiotics has contributed significantly to the selection of antimicrobial resistant pathogens, as well as the disruption of beneficial microbiota.¹ To mitigate these growing problems, stimuli-responsive drug-delivery systems, initially developed for cancer therapy, are now also being utilized for on-demand antimicrobial delivery applications.² One such technology involves the use of hydrogels that can deliver drugs, on-demand, upon light activation.^{3,4} Light is an ideal external stimulus because of its non-invasive nature and the ease by which it can be spatially and temporally controlled.^{5,6} Light-responsive drug delivery systems thus allow for explicit control over where and when, and to some degree how much, antimicrobials are released—ideal for treating localized infections such as those found in chronic wounds, dental plaques and in medically implanted devices.^{7,8}

Photothermal activation is one of the most common strategies used for light-activated, hydrogel-based drug delivery systems.⁵ Here, photothermally active materials, *i.e.*, those that generate heat upon photoexcitation, are incorporated in the

hydrogel matrix to stimulate thermally sensitive drug-carrying components, eventually triggering cargo release. Recently, hybrid platforms such as nanocomposite hydrogels, where hydrogels and photoactive nanoparticles are combined, have been used for light-activated drug delivery applications.^{9,10} While gold nanoparticles are commonly used, other photo-thermally active nanomaterials, like the bioinspired polydopamine nanoparticles (PDNP), have also been increasingly utilized.^{11–13} PDNP can additionally serve as a carrier for various drug molecules as its surface can readily be functionalized.¹⁴ PDNP has therefore been extensively studied not only for cancer therapy but also for antimicrobial applications.^{15–17}

Here we leverage on the photoactivity of PDNP,¹⁸ the temperature-dependent properties of liposomal carriers,¹⁹ and the flexibility afforded by nanocomposite hydrogels—to engineer a laser-responsive, on-demand, drug-delivery system for adjunctive therapy. With this platform, we are able to deliver—in a sequential manner—a membrane potentiator, ethylenediaminetetraacetic acid (EDTA), followed by the large hydrophobic drug, rifampicin. We further show that this laser-activated, sequential delivery is effective towards inhibiting the growth of Gram-negative bacteria. Gram-negative bacteria, unlike Gram-positive microorganisms, have robust outer membranes that make them impermeable to large hydrophobic drugs. This makes them naturally resistant to many antibiotics, like rifampicin, which are more effective against Gram-positive pathogens.^{20,21} As a membrane permeabilizer, EDTA primes the bacterial envelope of Gram-negatives such as *E. coli*, making them more susceptible to rifampicin treatment.²² Controlled delivery of adjunctive therapies, such as the one developed here, could therefore help increase the efficacy of currently available antibiotics against mixed-species and drug-resistant bacterial infections.^{23–25}

The smart nanocomposite hydrogel in our work consists of two thermally responsive liposomal nanocarriers of distinct lamellarity, and PDNP, embedded in a low gelling temperature agarose hydrogel (Scheme 1A). The first liposome, dipalmitoylphosphatidylcholine (DPPC) unilamellar vesicles (ULV), were

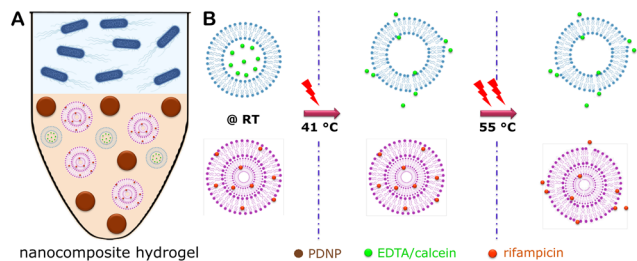
^aDepartment of Physical and Environmental Sciences, University of Toronto Scarborough, 1065 Military Trail, Toronto, Ontario, M1C 1A4, Canada.
E-mail: ruby.sullan@utoronto.ca

^bDepartment of Chemistry, University of Toronto, 80 St. George St., Toronto, Ontario, M5S 3H6, Canada

† Electronic supplementary information (ESI) available. See DOI: <https://doi.org/10.1039/d2bm01471h>

‡ These authors contributed equally.

§ Present address: Department of Chemical Engineering and Biotechnology, University of Cambridge, Philippa Fawcett Drive, Cambridge, UK, CB3 0AS.



Scheme 1 Laser-responsive smart hydrogel for sequential drug release. (A) Schematic for a nanocomposite hydrogel showing EDTA/calcein (green spheres)-loaded unilamellar vesicles (blue), rifampicin (red spheres)-loaded multilamellar vesicles (purple), and the photothermally active polydopamine nanoparticles (PDNP, brown spheres), embedded in an agarose hydrogel. Bacterial solution (blue rods) sits on top of the hydrogel. (B) Laser-induced temperature dependent sequential release of EDTA/calcein (at 41 °C) followed by rifampicin (at 55 °C).

loaded with EDTA, while the second liposome, distearoylphosphatidylcholine (DSPC) multilamellar vesicles (MLV), were loaded with rifampicin (Scheme 1, ESI sections 1–2 and Fig. S1–S4†). The presence of the photoactive PDNP allows us to use a laser to raise the temperature of the system to the transition temperatures (T_m) of each liposome, *i.e.*, 41 °C and 55 °C for DPPC and DSPC, respectively. Once T_m is reached, the liposomes transition from an ordered gel to a more fluid liquid crystalline phase, loosening the lipid packing and allowing the cargo to be released (Scheme 1B).¹⁹ The broad absorption spectrum of PDNP enabled the use of a NIR laser (808 nm), which allows for maximum tissue penetration while minimizing light-induced tissue heating.²⁶

As a control, we first verified the temperature dependent cargo release from the nanocomposite hydrogel using an external heater (ESI section 1†). Cargoes that escaped from the liposomes and diffused into the solution on top of the gel were quantified using absorption spectroscopy (Scheme 1A and Fig. S5†). While rifampicin (being a chromophore) can be directly quantified, quantifying the release of EDTA is not straightforward. As such, calcein-loaded DPPC ULV was used instead. Calcein has the same number of carboxylate groups as EDTA yet contains a fluorescein chromophore that can be used for direct quantification of cargo release (Fig. S2A†).

The externally-heated, temperature-dependent cargo release from the nanocomposite hydrogels is shown in Fig. 1. When the hydrogel was heated to 25 °C, calcein-loaded DPPC ULVs remained stable (Fig. 1A-blue spheres). Minimal amount of calcein release was observed, which plateaus after ~15 min of incubation, evident from the absorption spectra that quickly saturates within this timeframe (Fig. 1A inset-blue). As the calcein-loaded DPPC in the hydrogel remained stable for several days at 25 °C (Fig. S6A†), this observed minimal release could be attributed to calcein molecules that escaped from the liposomes during gel preparation—and not while the gel is incubating at 25 °C. When the temperature was raised to the T_m of DPPC (41 °C), a drastic increase in absorption was observed (Fig. 1A inset-green), resulting from ~8× more calcein

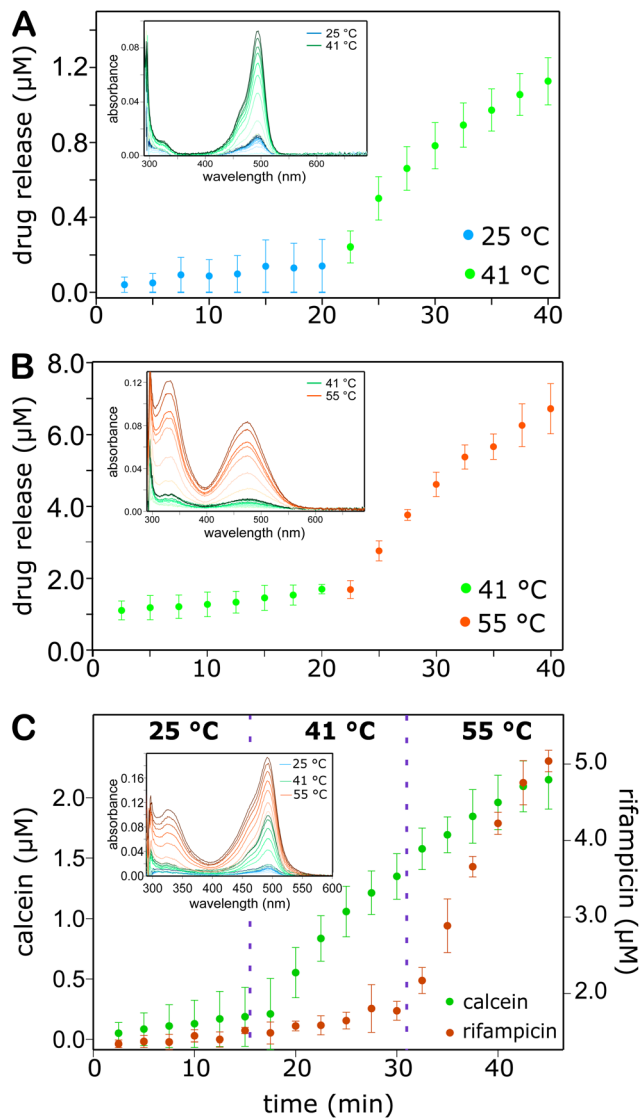


Fig. 1 Temperature dependent drug release. Amount of cargo released from hydrogels embedded with (A) calcein-loaded DPPC ULVs incubated at 25 °C and 41 °C, (B) rifampicin-loaded DSPC MLVs at 41 °C and 55 °C, and (C) both calcein-loaded DPPC ULVs and rifampicin-loaded DSPC MLVs at 25 °C, 41 °C and 55 °C. Insets: spectra of (A) calcein, (B) rifampicin, and (C) calcein and rifampicin released from the nanocomposite hydrogels, taken at 2.5 min interval.

diffusing out of the gel within only 20 min. We further verified that this increase in calcein concentration is not a result of liposomes escaping from the gel matrix, but rather due to calcein escaping from the liposomes and diffusing out of the gel at 41 °C (Fig. S7†).

For sequential delivery to be successful, it is critical to ensure that rifampicin-loaded DSPC liposomes do not inadvertently release the drug at 41 °C, while the EDTA/calcein-loaded DPPC liposomes are releasing their cargo. Fig. 1B shows that for rifampicin-loaded DSPC MLVs, molecules released at 41 °C was minimal (Fig. 1B inset-green), but steeply increased when the temperature was raised to the T_m of DSPC (55 °C) (Fig. 1B

inset-orange). We further verified that this drastic increase in the amount of rifampicin is not due to MLVs leaking out of the hydrogel, but rather due to rifampicin escaping from MLVs and diffusing out of the gel after the hydrogel was heated at 55 °C (Fig. S7†). Furthermore, like the cargo-loaded DPPC liposomes, these rifampicin-loaded DSPC liposomes remain stable in the hydrogel both at 4 °C and 25 °C, with no significant cargo leakage observed for up to 6 days (Fig. S6B†).

When both rifampicin- and calcein-loaded vesicles are embedded in the same hydrogel, temperature dependent cargo release was still observed. Fig. 1C-inset displays the spectra of the solution above the gel as it is heated from 25 °C to 41 °C, then to 55 °C. From these spectra, we can calculate how much calcein and rifampicin were released into the solution during equilibration at each temperature. Fig. 1C inset-blue shows that both liposomes remained stable at 25 °C, resulting in very minimal amounts of both calcein and rifampicin released from the hydrogel (Fig. 1C, $t = 0-15$ min). Similar to hydrogels containing only one type of liposome, these molecules that diffused out were most likely released within the gel matrix during hydrogel formation, as both liposomes can retain their cargo for days at 25 °C (Fig. S6†). When the temperature was raised to 41 °C (Fig. 1C, $t = 15-30$ min), the absorbance of the solution drastically increased with time. Furthermore, the spectra at 41 °C resemble that of calcein, with the 495 nm peak increasing while the peak at 335 nm remains relatively constant (Fig. 1C inset-green). From these spectra, the calculated amount of each molecule shows minimal change in the amount of rifampicin diffusing out at 41 °C, with the average rate increasing by only $\sim 1.4\times$ within the 15 min timeframe, while calcein was diffusing out $\sim 9\times$ faster at 41 °C than at 25 °C. When the temperature was further raised to 55 °C, peaks at 335 nm and 495 nm increased significantly (Fig. 1C inset-orange), indicating the release of rifampicin in addition to calcein. The total amount of each molecule that contributed to the overall spectrum was again calculated and shown in Fig. 1C from 30 min onwards. On average, the rate of rifampicin release from the gel is $\sim 13\times$

faster at 55 °C than at 41 °C. Though the rate of diffusion also increases with increasing temperature, the relatively similar kinetics of rifampicin release at 25 °C and 41 °C implies that the temperature dependent drug release observed here is largely driven by the temperature responsive properties of the liposomal drug carriers, and not mainly due to temperature dependent diffusion.

Having shown that temperature dependent cargo release persisted when both liposomes are embedded in the same hydrogel, we then tested the efficacy of the sequential release on inhibiting the growth of a drug-resistant strain of *E. coli*, AR3110.²⁷ Here, bacterial solution was placed on top of the hydrogel (Scheme 1A) and treated under five different conditions: (1) control (no treatment), (2) hydrogel only (heat treated with no drug-loaded liposomes) (3) heat + rifampicin-loaded liposomes, (4) heat + EDTA-loaded liposomes, and (5) heat + EDTA- and rifampicin-loaded liposomes. Heat treatment involves external heating at 41 °C (2 min) and 55 °C (2 min), using water baths. Fig. 2A summarizes the effect of each treatment on the growth of *E. coli* in M9 minimal media with 0.05 mM Ca^{2+} and 0.5 mM Mg^{2+} . These growth curves were then fitted with the Gompertz equation to obtain growth parameters. The effect of different treatments on the growth rate of *E. coli* is shown in Fig. 2B. Fig. 2 (2) shows that heat treatment alone can already partially inhibit bacterial growth compared to control, suggesting that the current heating conditions contribute to bacterial growth inhibition. We further verified that this is mainly due to heating at 55 °C, as bacterial growth was slightly inhibited after just 2 min of exposure at 55 °C, while no growth inhibition was observed even after 10 min of exposure at 41 °C (Fig. S8†). However, 2 min of heating at 55 °C is not enough to completely prevent *E. coli* from growing (Fig. S8†). A similar trend was observed for the heat-induced release of rifampicin from hydrogels containing only rifampicin-loaded liposomes. Fig. 2 (3) shows that there was only partial growth inhibition, indicating that the amount of rifampicin released under these conditions is not enough to completely inhibit *E. coli* growth, a scenario which mimics low bio-

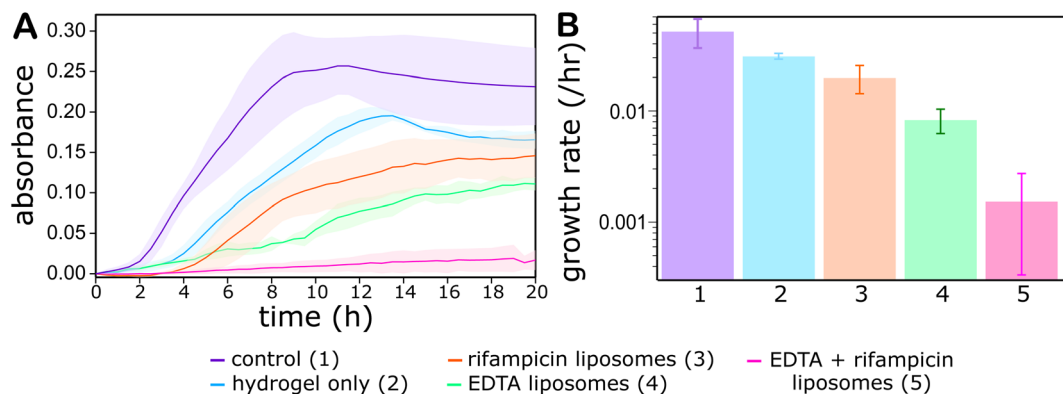


Fig. 2 Effect of sequential release of EDTA and rifampicin on *E. coli* growth. (A) Growth curves for *E. coli* with no treatment control (purple) and treatment with no liposomes (blue), only rifampicin-loaded liposomes (orange), only EDTA-loaded liposomes (green), and both EDTA- and rifampicin-loaded liposomes (pink) in a hydrogel. (B) Corresponding growth rate obtained by fitting the growth curves in A with the Gompertz function.

availability of these types of hydrophobic drug molecules. We note that the current heat treatment does not affect how rifampicin inhibits the growth of *E. coli* (Fig. S9A†), which indicates that the inhibition we observed in Fig. 2 (3) is mainly due to the action of rifampicin. Next, we tested how bacterial growth is affected upon heat-induced EDTA release from the hydrogels. Fig. 2 (4) shows more growth inhibition, with ~ 6 -fold decrease in growth rate *vs.* control, after heat + EDTA treatment. While EDTA alone can inhibit *E. coli* growth,²⁸ heat makes *E. coli* even more susceptible to EDTA treatment (Fig. S9B†), possibly due to the effect of heat on the release of outer membrane fragments upon EDTA treatment.²⁹ However, despite the more effective inhibition with temperature-induced release of EDTA, an even more drastic decrease in growth rate, ~ 34 -fold, was observed when hydrogels containing both EDTA- and rifampicin-loaded liposomes were used. Other growth parameters (*i.e.*, lag time and maximum growth) were also more affected when *E. coli* was treated with both EDTA and rifampicin (Fig. S10†). This suggests that controlled co-delivery of an antibiotic and its adjuvant can indeed help towards a more effective control of pathogen proliferation.

Using an external heating device for controlling the temperature of drug-delivery systems is quite challenging. For this reason, the use of the photothermally active PDNP makes temperature control more feasible. By using laser as the light source, the temperature of PDNP-containing hydrogel systems can easily be tuned, with high spatial and temporal resolution.^{11–13} By simply adjusting the laser power, we can

control the temperature of the nanocomposite hydrogel system, *i.e.*, agarose hydrogel + PDNP + cargo-loaded liposomes (Fig. 3A and Fig. S11†). In the presence of PDNP, laser can therefore be used to control the temperature-dependent cargo release from the gel (Fig. 3B), akin to systems using an external heat source (Fig. 1). When the gel was maintained at room temperature (~ 25 °C), minimal cargo release was observed (Fig. 3B-blue). Upon adjusting the laser power (214 mW), enough to heat the laser illuminated area to ~ 41 °C, a strong peak at 495 nm is observed, suggesting calcein release. Moreover, the absorbance at 335 nm remains low, suggesting that rifampicin loaded liposomes remained mostly intact. Further increase in laser power (412 mW), to ~ 53 °C hydrogel temperature, the peak at 335 nm starts to increase, indicating that rifampicin was also being released from the gel. The high spatial resolution afforded by using laser irradiation and the localized heating near the surface of nanoparticles enabled us to use lower laser power (only enough to heat a small area to ~ 53 °C) and still induced cargo release from rifampicin-loaded DSPC MLVs. Thus, by simply controlling the laser power and irradiation time, we can achieve the sequential release of different molecules, encapsulated within different liposomes, from this PDNP-loaded nanocomposite hydrogel.

After establishing laser-controlled cargo release, the efficacy of the nanocomposite hydrogel towards antimicrobial application was next tested. Here, rather than using calcein, EDTA-loaded liposomes were incorporated in the gel, together with

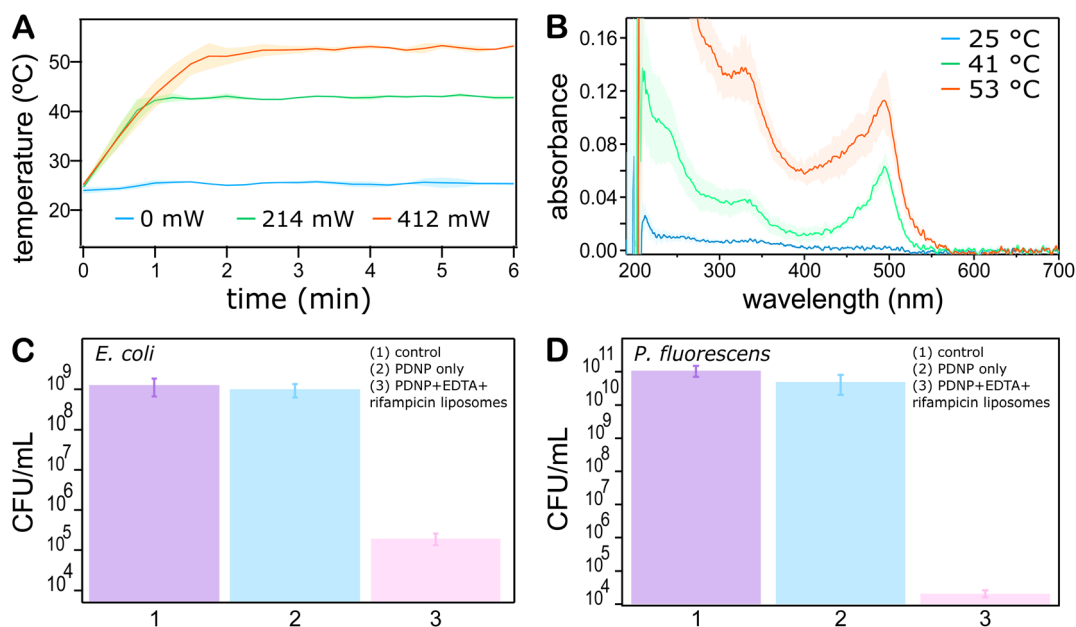


Fig. 3 Laser-induced sequential drug release. (A) Laser irradiation of PDNP-liposome nanocomposite hydrogel was used with the laser powers adjusted to achieve temperatures of ~ 25 °C (blue), ~ 41 °C (green), and ~ 53 °C (orange). (B) The absorbance spectrum showing minimal drug release at ~ 25 °C (blue), a peak corresponding to calcein release at ~ 41 °C (green), and a peak corresponding to rifampicin release at ~ 53 °C (orange). (C and D) Effect of laser-induced sequential delivery of EDTA and rifampicin from PDNP-loaded nanocomposite hydrogels on colony forming units (CFU mL⁻¹) of *E. coli* (C) and *P. fluorescens* (D): (1) control (w/o laser), (2) no liposomes (w/laser), and (3) EDTA and rifampicin liposomes (w/laser).

rifampicin-loaded liposomes and PDNP. *E. coli* growth inhibition was then monitored for 20 hours following laser-controlled drug delivery (Fig. S12A†). Compared to control, the growth rate was inhibited by ~26-fold after laser-induced sequential release of EDTA and Rifampicin (Fig. S12B†). To further quantify the growth inhibiting effect of rifampicin on the EDTA-primed *E. coli*, the number of colony forming units (CFU) was obtained after allowing the laser-treated bacterial solution to grow for 20 h. Fig. 3C highlights the bacterial growth inhibiting effect of the treatment, as ~10⁴-fold decrease in the number of CFU was observed after 20-hr growth period (Fig. S12B and S13A†). This indicates that the laser-induced sequential release of EDTA and rifampicin successfully prevented the growth of *E. coli*. As rifampicin is a known bacteriostatic but not bactericidal, the treated bacteria started growing into colonies when rifampicin and EDTA were removed during CFU counting assay where bacteria solution was transferred on an LB agar.

We further tested the effect of laser-induced heating of hydrogels on bacterial viability using hydrogels containing only PDNP, without the drug-loaded liposomes. This laser-induced heating, localized within the laser illuminated area in the hydrogel, have minimal effect on the growth of *E. coli* (Fig. 3C (2)). This is in contrast to what was observed when heating using the water bath, where external heating (alone) of the whole system did have a significant effect on the growth of *E. coli*. It has been shown recently that the heat generated by at least 10 min of photothermal therapy can cause antibiotic tolerance in *E. coli* by inducing cells into a low energy state.³⁰ We have shown that with this hydrogel-based antimicrobial delivery platform, we can reduce this heat-related risks, as laser-induced heating can be localized within the hydrogel, in the vicinity of the laser-heated nanoparticles. Furthermore, the highly temperature-sensitive nature of liposomal drug carriers allowed for a short laser irradiation time (2 min, Fig. S11†), limiting the exposure of bacteria to heat, potentially preventing the induction of antibiotic tolerance.

The effectivity of this laser-controlled multi-drug delivery system was also tested using another species of Gram-negative bacteria, *Pseudomonas fluorescens* (strain WCS374). Similar to *E. coli*, growth inhibition of *P. fluorescens* (~10⁶-fold) was observed after the laser-induced sequential release of EDTA and rifampicin from the hydrogel (Fig. 3D and Fig. S13B†). This suggests that this laser-responsive drug delivery platform has the potential to be applied to other Gram-negative bacteria, and points to the general applicability of this nanocomposite hydrogel system. Furthermore, future developments for these photothermal drug delivery systems could explore changing lipid compositions or using polymer modified liposomes to expand the repertoire of nanocarriers with different and lower transition temperatures.^{31,32} This will lead to not only an increase in the number of antimicrobials that can be co-delivered, but could also limit the adverse effects of high temperatures on healthy cells, making it promising for potential *in vivo* applications such as treatment of localized infections found in chronic wounds and in dental caries.^{33,34}

Conclusions

A nanocomposite hydrogel (containing the highly efficient photoactive agent, PDNP, and temperature-responsive liposomal drug carriers) is used as a light-activated multi-drug delivery platform. As a proof-of-principle, we used this platform for the on-demand, laser-responsive delivery of an antibiotic, rifampicin, and a membrane potentiator, EDTA. This adjunctive therapy was successful in preventing the proliferation of Gram-negative bacteria. The modular nature of this system allows for flexibility that has the potential to expand its application to other adjunctive therapy combinations or delivery of multiple antimicrobials, including other antibiotics, as well as antimicrobial peptides and polymers.

Conflicts of interest

There are no conflicts to declare.

References

- R. Laxminarayan, A. Duse, C. Wattal, A. K. M. Zaidi, H. F. L. Wertheim, N. Sumpradit, E. Vlieghe, G. L. Hara, I. M. Gould, H. Goossens, C. Greko, A. D. So, M. Bigdeli, G. Tomson, W. Woodhouse, E. Ombaka, A. Q. Peralta, F. N. Qamar, F. Mir, S. Kariuki, Z. A. Bhutta, A. Coates, R. Bergstrom, G. D. Wright, E. D. Brown and O. Cars, *Lancet Infect. Dis.*, 2013, **13**, 1057–1098.
- S. Mura, J. Nicolas and P. Couvreur, *Nat. Mater.*, 2013, **12**, 991–1003.
- J. Y. Li and D. J. Mooney, *Nat. Rev. Mater.*, 2016, **1**, 16071.
- A. Vashist, A. Vashist, Y. K. Gupta and S. Ahmad, *J. Mater. Chem. B*, 2014, **2**, 147–166.
- C. S. Linsley and B. M. Wu, *Ther. Delivery*, 2017, **8**, 89–107.
- Y. Tao, H. F. Chan, B. Y. Shi, M. Q. Li and K. W. Leong, *Adv. Funct. Mater.*, 2020, **30**(49), 2005029.
- P. K. Kundu, D. Samanta, R. Leizrowice, B. Margulis, H. Zhao, M. Borner, T. Udayabhaskararao, D. Manna and R. Klajn, *Nat. Chem.*, 2015, **7**, 646–652.
- V. Shanmugam, S. Selvakumar and C. S. Yeh, *Chem. Soc. Rev.*, 2014, **43**, 6254–6287.
- P. Lavrador, M. R. Esteves, V. M. Gaspar and J. F. Mano, *Adv. Funct. Mater.*, 2021, **31**(8), 2005941.
- S. C. T. Moorcroft, L. Roach, D. G. Jayne, Z. Y. Ong and S. D. Evans, *ACS Appl. Mater. Interfaces*, 2020, **12**, 24544–24554.
- N. Falcone, N. M. O. Andoy, R. M. A. Sullan and H. B. Kraatz, *ACS Appl. Bio Mater.*, 2021, **4**, 6652–6657.
- A. GhavamiNejad, M. SamariKhalaj, L. E. Aguilar, C. H. Park and C. S. Kim, *Sci. Rep.*, 2016, **6**, 33594.
- X. Wang, C. P. Wang, X. Y. Wang, Y. T. Wang, Q. Zhang and Y. Y. Cheng, *Chem. Mater.*, 2017, **29**, 1370–1376.
- J. H. Ryu, P. B. Messersmith and H. Lee, *ACS Appl. Mater. Interfaces*, 2018, **10**, 7523–7540.

- 15 Y. Fu, L. Yang, J. H. Zhang, J. F. Hu, G. G. Duan, X. H. Liu, Y. W. Li and Z. P. Gu, *Mater. Horiz.*, 2021, **8**, 1618–1633.
- 16 I. Matai, M. Garg, K. Rana and S. Singh, *RSC Adv.*, 2019, **9**, 13444–13457.
- 17 R. Mrowczynski, *ACS Appl. Mater. Interfaces*, 2018, **10**, 7541–7561.
- 18 Y. L. Liu, K. L. Ai, J. H. Liu, M. Deng, Y. Y. He and L. H. Lu, *Adv. Mater.*, 2013, **25**, 1353–1359.
- 19 G. Cevc, *Biochemistry*, 1991, **30**, 7186–7193.
- 20 A. H. Delcour, *BBA, Proteins Proteomics*, 2009, **1794**, 808–816.
- 21 G. Kapoor, S. Saigal and A. Elongavan, *J. Anaesthesiol., Clin. Pharmacol.*, 2017, **33**, 300–305.
- 22 P. Reid and J. Speyer, *J. Bacteriol.*, 1970, **104**(1), 376–389.
- 23 V. J. Morley, C. L. Kinnear, D. G. Sim, S. N. Olson, L. M. Jackson, E. Hansen, G. A. Usher, S. A. Showalter, M. P. Pai, R. J. Woods and A. F. Read, *eLife*, 2020, **9**, e59174.
- 24 R. J. Melander and C. Melander, *ACS Infect. Dis.*, 2017, **3**, 559–563.
- 25 U. Theuretzbacher, K. Outtersson, A. Engel and A. Karlen, *Nat. Rev. Microbiol.*, 2020, **18**, 275–285.
- 26 S. Pearson, J. Feng and A. del Campo, *Adv. Funct. Mater.*, 2021, **31**(50), 2105989.
- 27 N. M. O. Andoy, K. Jeon, C. T. Kreis and R. M. A. Sullan, *Adv. Funct. Mater.*, 2020, **30**, 2004503.
- 28 C. Pelletier, P. Bourlioux and J. Vanheijenoort, *FEMS Microbiol. Lett.*, 1994, **117**, 203–206.
- 29 H. J. P. Marvin, M. B. A. Terbeest and B. Witholt, *J. Bacteriol.*, 1989, **171**, 5262–5267.
- 30 Y. Qiu, S. M. Yu, Y. L. Wang, L. Y. Xiao, L. S. Pei, Y. Y. Pu and Y. F. Zhang, *Biomater. Sci.*, 2022, **10**, 1995–2005.
- 31 G. R. Anyarambhatla and D. Needham, *J. Liposome Res.*, 1999, **9**(4), 491–506.
- 32 M. Bikram and J. L. West, *Expert Opin. Drug Delivery*, 2008, **5**, 1077–1091.
- 33 L. P. Zhou, T. T. Min, X. C. Bian, Y. Z. Dong, P. X. Zhang and Y. Q. Wen, *ACS Appl. Bio Mater.*, 2022, **5**, 4055–4085.
- 34 T. Zhu, Z. Y. Huang, X. Y. Shu, C. L. Zhang, Z. Q. Dong and Q. Peng, *Colloids Surf. B*, 2022, **218**, 112761.